Transferable potential for carbon without angular terms

Jeremy Q. Broughton
Complex Systems Theory Branch, Naval Research Laboratory, Washington, D.C. 20375
and Yale School of Management, 135 Prospect Street, P.O. Box 20820, New Haven, Connecticut 06520

Michael J. Mehl
Complex Systems Theory Branch, Naval Research Laboratory, Washington, D.C. 20375
(Received 10 September 1998)

A simple transferable potential for carbon is developed for use in atomistic simulation. It describes all the phases of carbon, from the close packed, such as face centered cubic, to the open systems, such as diamond cubic, graphite, and even linear chains. The parameters are fit to a total-energy local-density functional theory database augmented by the known cohesive energies of diamond and graphite. Further, structures such as simple molecules, not in the database, are well described. For example, it predicts that odd number of atom molecules form chains whereas even atom number molecules form rings. The diamond cubic and graphitic structures are dynamically stable. The formalism also allows for interaction with an external electric field. Further, it can be generalized to other covalent systems as well as mid-*d*-block elements.
[S0163-1829(99)00814-0]

I. INTRODUCTION

Carbon, besides being the basis for all organic chemistry, displays amazingly varied and important materials properties: from the structural and radiation hardness implicit in diamond, to its lubricating and conducting properties in graphite, to its novel strength coupled with electronic and encapsulating abilities in the fullerenes. Much has been learned and predicted about carbon by using atomistic simulation whether such was at the purely empirical potential or at the fully *ab initio* level.

The list of successes in the simulation of carbon is too long to be addressed properly here. Suffice it to give some representative examples: The relative energies of different crystalline forms of carbon have been obtained by local-density functional (LDA) calculations.[1,2] LDA molecular-dynamics (MD) calculations have elucidated the structure of liquid[3] and amorphous[4] carbon. LDA calculations,[5] and atomistic potentials for the intramolecular interactions,[6,7] have evaluated and predicted vibrational modes in C_{60} molecules very accurately. Semiempirical tight-binding (TB) simulations have predicted stabilities of whole families of fullerenes.[8] Empirical potential MD simulations have predicted the C_{60} phase diagram.[9] LDA calculations have assisted our understanding of fullerene polymerization.[10] TB MD simulations have investigated the effects of helicity on the phonon modes in fullerene tubules.[11] First-principles and TB methods have studied the electronic effects due to dopants in diamond.[12–15] And last, high quality quantum chemical calculations have addressed the nature of small carbon clusters.[16]

Such is carbon's centrality to materials science; it would be useful to have a robust transferable interatomic potential which allows the description of carbon in its many guises: the fourfold coordination of diamond, the threefold coordination of graphite and the fullerenes, and the twofold nature of simple carbon molecules. Here we develop such a potential, which has utility with the high coordination (and therefore high-energy) structures also.

Most extant interatomic potentials for covalent systems make use of molecular-orbital concepts. Examples include Stillinger and Weber,[17] Tersoff,[18] Biswas and Hamann,[19] Chelikowski and co-workers,[20–22] and Bazant, Kaxiras, and Justo[23] for silicon. Another example is the extremely useful interatomic potential for carbon, due to Brenner,[24] which uses the concept of bond order to allow description of graphite and diamond. The strength of a bond, here, is a function of its environment. These ideas have been generalized and placed on a firm theoretical footing by Pettifor and co-workers[25,26] such that the concept of bond order applies to a wide range of systems.

In developing the present interatomic potential we make use of two other concepts—that of the valence bond (VB) and that of the radius ratio. Both of these ideas owe their lineage to Pauling.[27] The radius ratio rules explain why some ionic systems choose to crystallize with eight nearest neighbors while others choose six or four (or even three or two). The rules are derived from hard-sphere packing arguments which rely upon the idea that ionic radii are transferable and that smaller cations fit in the interstices of the larger anion lattice. (Usually, the cations are smaller than the anions.) The interstice size must be as small as possible and yet still be able to accommodate the cation. The valence bond concept involves representing the electronic structure of a system as a linear combination of contributing states. The best example of this is in the Kekule structures for benzene.

That these ideas might work well for pure carbon is illustrated thus. Behrman *et al.*[28] observed, while trying to find the ground state of ZnO clusters, that rather than relaxing to structures related to truncations of the bulk zinc blende lattice, fullerene structures were found instead. Apparently, within the language of radius ratios, the cation to anion size ratio for ZnO is such that it lies on the borderline between threefold and fourfold coordination. Table I gives the stabil-

TABLE I. Radius ratio ranges and examples of structure types. bcc represents body centered cubic; sc represents simple cubic; DC represents diamond cubic; Gr. represents graphite; and chain represents a linear chain.

r_+/r_-	Coord.	Structure	Lattice
1.000–0.732	8	CsCl	bcc
0.732–0.414	6	NaCl	sc
0.414–0.225	4	ZnS	DC
0.225–0.155	3	BN	Gr.
0.155–0.000	2 or 1	$(SN)_x$	chain

ity ranges of radius ratios for different structures. (Table I also defines shorthand notation for different structures.) In a bulk system, perhaps it is the Madelung field which flips the packing decision away from threefold towards fourfold coordination. Madden and co-workers[29] have used these ideas to great effect in the study of mixed ionic/covalent systems. In their formalism, a full integer charge equal to the formal oxidation state is assigned to each ion. The ions are then taken to be polarizable and are assigned point dipole and quadrapole moments as dynamical variables. In this way several different phases of ionic/covalent systems may be described.

In applying similar ideas to carbon, we note that carbon sits in the middle of the square planar (sp) block. It is an amphoteric atom; that is it has intermediate electronegativity and may be atomically positively or negatively charged depending upon the chemical nature of the atoms to which it is bonded. In other words, carbon atoms are capable of donating or accepting electrons. We note that carbon has two phases of almost identical stability under ambient conditions—namely diamond and graphite. Thus one way of thinking about carbon is that it sits on a similar stability border as the ZnO example given above—that is, if only it had an ionic radius. We may impart an ionic radius to carbon by taking advantage of its amphoteric nature and by employing a valence bond description. In a lattice without frustration we may, to first order, consider assigning half the atoms a charge of $+q$ and the other half a charge of $-q$. But since the atoms in pure carbon should be indistinguishable and carry no charge we take a linear combination of this state with the equivalent one (energetically) in which all identities have been switched; this is the valence bond concept. Other charge distributions will, of course, contribute to a VB description, such as those in which charges are no longer atom centric, but for the sake of simplicity aimed at pursuing the impact of the radius ratio concept, we chose initially to confine our attention to ionic distributions.

All that remains is to formulate a physically intuitive functional form for our picture of bonding in carbon and also to fit the free parameters in such to a database. Unlike the formulation of Wilson and Madden,[29] our dynamical variables are taken to be the charges $\{q\}$ in the system—dipole and quadrapole moments are not used. In Sec. II we describe the functional form to which we will fit and also the raw data generated by LDA calculations. In Sec. III we employ our Hamiltonian to examine the dynamical stability of diamond and graphite. Also we show that the Hamiltonian correctly predicts that even number atom carbon molecules will form rings while odd number atom systems do not. Section IV presents our conclusions as well as suggestions as to how such a Hamiltonian might be applied to disordered (i.e., frustrated) systems such as amorphous and liquid carbon. We further suggest that this formalism will generalize simply to other covalent systems such as silicon, to mid-*d*-block elements and to systems in the presence of an electrostatic field. The latter will be particularly useful for fullerene tubules which are often grown under high-field conditions.

II. FUNCTIONAL FORM

We wish to be able to describe high coordination metallic systems as well as the low coordination covalent systems. For the former, we expect an embedded atom (EAM) description[30,31] to be good. For the latter, we anticipate our linear combination of degenerate ionic representations will work well. Thus we require a scheme which interpolates between these two extremes depending upon atomic structure.

The simplest approximation that has this interpolative quality is to solve for the energy (E_{VB}) of the system from the following determinant. It borrows, as we have said, from concepts within VB theory. Although, within the development of the present Hamiltonian, such VB expansion is not rigorous, we shall henceforth use VB terminology to imply the mixing of contributing states:

$$\begin{vmatrix} (H_E - E_{VB}) & (H_{EC} - E_{VB}S_{EC}) \\ (H_{EC} - E_{VB}S_{EC}) & (H_C - E_{VB}) \end{vmatrix} = 0. \tag{1}$$

The solution is

$$E_{VB} = \frac{[\frac{1}{2}(H_C + H_E) - S_{EC}H_{EC}]}{(1 - S_{EC}^2)} \pm \frac{[\frac{1}{4}(H_C - H_E)^2 + (S_{EC}H_E - H_{EC})(S_{EC}H_C - H_{EC})]^{1/2}}{(1 - S_{EC}^2)}. \tag{2}$$

The H_E term represents the energy of the system when all atoms are neutral and described by an EAM Hamiltonian. The H_C term is the energy of the ionic (Coulomb) representation of the system. For the simple ordered structures in our database, we will *assume* that only the lowest energy (i.e., dominant) distribution of charges contributes. Thus for fcc we use a TiAl (see below) arrangement of charges; for bcc we use CsCl; for simple cubic (sc) we use NaCl; for diamond cubic (dc) we use ZnS; for graphite (Gr.) we use BN, and for the linear chain (chain) we use $(SN)_x$ (see Table I). Actually, in the case of graphite, the basal plane stacking is not identically that of BN—there is a lateral shift of one relative to another. Such is the charge transfer in true BN, the boron of one layer prefers to sit directly above a nitrogen in the layer beneath. This is not true in graphite; atoms sit above the hexagonal hollow of the layer beneath. In our database, to account for such energetic differences, we have calculated the total energies of hexagonal carbon in both the true graphitic *and* BN stackings (see Tables II and III).

The form of H_E is that advocated by Johnson and Oh:[32]

TABLE II. LDA energy database for graphite (with graphitic stacking) and for orthorhombic distortions. Energy given in rydbergs per unit cell. Distances in bohr. Four atoms/cell.

a_1	a_2	a_3	Energy
4.20		7.00	−301.810522
4.20		7.50	−301.974497
4.20		8.00	−302.092591
4.20		8.50	−302.171984
4.20		9.50	−302.255620
4.20		10.50	−302.287088
4.30		7.00	−301.914106
4.30		7.50	−302.071556
4.30		8.00	−302.187328
4.30		8.50	−302.267314
4.30		9.50	−302.352279
4.30		10.50	−302.384850
4.40		8.00	−302.250926
4.40		8.50	−302.330777
4.40		9.00	−302.383258
4.40		9.50	−302.416745
4.40		10.50	−302.450213
4.50		8.50	−302.367080
4.50		9.00	−302.419785
4.50		9.50	−302.453716
4.50		10.00	−302.475007
4.50		10.50	−302.487902
4.60		10.50	−302.502134
4.60		11.50	−302.513776
4.60		12.50	−302.515853
4.60		13.50	−302.514758
4.63		13.470	−302.515226
4.70		10.502	−302.496220
4.70		11.506	−302.508253
4.70		13.505	−302.509636
4.18726	5.11776	13.47096	−302.366606
4.31573	4.96541	13.47096	−302.442370
4.40324	4.86674	13.47096	−302.476848
4.86674	4.40324	13.47096	−302.473846
4.96541	4.31573	13.47096	−302.435900
5.11776	4.18726	13.47096	−302.362061

$$H_E=\sum_{ij}\ \phi_{eam}(r_{ij})-\lambda\sum_i\ \left[1-\ln\left(\frac{\rho_i}{\rho_0}\right)^{\eta_r ho}\right]\left[\frac{\rho_i}{\rho_0}\right]^{\eta_{rho}}, \tag{3}$$

where i and j represent atom indices. Henceforth we use the convention that double sums exclude self-interaction terms and include unique pairs only. The pair EAM term is given by

$$\phi_{eam}(r_{ij})=\left[\alpha\left(\frac{2\sigma_0}{r_{ij}}\right)^{\eta_r}-\beta\left(\frac{2\sigma_0}{r_{ij}}\right)^{\eta_b}\right] \tag{4}$$

while ρ_i represents the background charge density in which atom i sits. It is obtained from a pairwise sum:

$$\rho_i=\sum_{j\neq i}\ e^{-\chi r_{ij}}. \tag{5}$$

TABLE III. LDA energy database for graphite (with boron nitride stacking) and linear chains. Two and one atoms/cell, respectively. Distances in bohr. Energy given in rydbergs per unit cell.

a_1	a_3	Energy
BN stacking		
4.6201238	5.82099625	−151.252402
4.6201238	6.02099625	−151.254336
4.6201238	6.22099625	−151.255612
4.6201238	6.32099625	−151.256029
4.6201238	6.42099625	−151.256325
4.6201238	6.52099625	−151.256520
4.6201238	6.62099625	−151.256637
Linear chain		
2.40184		−75.5355495620
2.41885		−75.5355262685
2.45664		−75.5338797346
2.54641		−75.5222224060

The form of H_C is

$$\begin{aligned}H_C=\frac{1}{2}\Bigg[&\sum_{AB}\ \phi_{+-}(r_{AB})+\sum_{AA}\ \phi_{++}(r_{AA})+\sum_{BB}\ \phi_{--}(r_{BB})\\&+\sum_{A}\ \phi_c(q^+)+\sum_{B}\ \phi_c(q^-)\Bigg]+\frac{1}{2}\Bigg[\sum_{AB}\ \phi_{-+}(r_{AB})\\&+\sum_{AA}\ \phi_{--}(r_{AA})+\sum_{BB}\ \phi_{++}(r_{BB})+\sum_{A}\ \phi_c(q^-)\\&+\sum_{B}\ \phi_c(q^+)\Bigg].\end{aligned} \tag{6}$$

We assume that, for given lattice structure, we have assigned some atoms an identity A and others an identity B. In the first half of this equation we have assigned positive charges to the A atoms and negative charges to the B atoms. The sum of the charges, of course, is zero. The second half of the equation implies that the signs of these charges have been flipped. The mean charge on each atom in the H_C Hamiltonian is thereby zero. The order of the $(+-)$ is important here. The first sign is applied to the charge on the first identity in the double sum while the second sign is applied to the charge on the second identity. ϕ_c (where c is either $+$ or $-$) represents the on-site electron affinity/ionization potential term:

$$\begin{aligned}\phi_+(q)&=U_+(q-q_0)^2-U_+q_0^2,\\ \phi_-(q)&=U_-(q-q_0)^2-U_+q_0^2.\end{aligned} \tag{7}$$

When q is more positive than q_0, the first of these equations in used. Otherwise the second is used. Thus, conforming with experiment, the on-site energy q dependence is that of an asymmetric parabola. The ϕ_c term is designed to have the value zero when the charge is zero. q_0 has a negative value since carbon has an electron affinity.

$\phi_{cc'}$ represents a Coulomb pairwise interaction term:

$$\phi_{cc'}(r_{LM})=\alpha\left(\frac{[\sigma(q_L)+\sigma(q_M)]}{r_{LM}}\right)^{\eta_{cc'}}+K\frac{q_L q_M}{r_{LM}}. \quad (8)$$

The indices L and M can be either A or B type atoms. The value of K is defined below. The constant α is positive and has the same value for both the H_E and H_C terms. The hard-core radii σ are small for cations and large for anions. In our fit, we constrain the ratio of these for the DC and Gr. structures in the database to be near the threefold to fourfold transition of Table I. Note that for reasons described below, the long-range Coulomb term is *not* damped. A linear dependence of $\sigma(q)$ is assumed:

$$\sigma_+(q)=\sigma_0+k_+q,$$

$$\sigma_-(q)=\sigma_0+k_-q. \quad (9)$$

σ_+ or σ_- is used depending upon the charge on atom L or M. σ_0 has the same value for both the H_E and H_C terms. q will be a parameter to be fit.

And finally, for the cross terms H_{EC} and S_{EC}, we have assumed:

$$S_{EC}=e^{-\gamma|q|},$$

$$H_{EC}=\frac{\varepsilon(|q|)}{2}(H_E+H'_C)S_{EC}e^{-\delta/N|H_E-H'_C|}, \quad (10)$$

where N is the total number of atoms in the system. The cross terms have the correct intuitive behavior. As the charge in the ionic state becomes large, we expect the overlap with the EAM state to become small. If S_{EC} becomes small, we expect H_{EC} to likewise decrease. As the energy difference between the Coulomb and EAM states becomes small, we expect the off-diagonal term to become large. And last, we expect H_{EC} to be proportional to some function of H_E and H_C; we chose to take the mean.

Note the prime modifying H_C in Eq. (10). To avoid pathologies as $|q|$ goes to zero, both ε and H_C must have specific behavior. First, ε must tend to unity as $|q|$ tends to zero, and second, the ionic contribution must tend to the EAM energy. Thus as $|q|$ tends to zero, the overall determinantal energy E_{VB} tends to the EAM energy. We chose

$$\varepsilon(|q|)=1+\epsilon|q|,$$

$$H'_C=H_Ee^{-\nu|q|}+H_C(1-e^{-\nu|q|}). \quad (11)$$

For the open structures such as the diamond, graphite, and linear chain where $|q|$ is expected to be large, H_C and H'_C should be almost equal.

It might be asked whether a van der Waals term should be included in the Hamiltonian. It is commonly thought that such a term accounts for most of the interlayer interaction in graphite. However, as we shall see, much of what holds graphite planes together is the (truncated) Madelung field of our VB Coulomb model. In our original fits an r^{-6} term was included in the Hamiltonian but we found it held negligible advantage. It has therefore been omitted from the final form. The final equation to which the data base is fit is

$$E_{VB}=\frac{[\frac{1}{2}(H'_C+H_E)-S_{EC}H_{EC}]}{(1-S_{EC}^2)} \pm\frac{[\frac{1}{4}(H'_C-H_E)^2+(S_{EC}H_E-H_{EC})(S_{EC}H'_C-H_{EC})]^{1/2}}{(1-S_{EC}^2)}, \quad (12)$$

where we use the solution with the lowest energy.

Finally, so as to make these functional forms computationally efficient, every pair term in the above equations is truncated to zero at a cutoff distance r_c which will be a parameter in the fit. Thus the $\phi_{cc'}$, $e^{-\chi r}$, and ϕ_{eam} terms are truncated as follows:

$$f_c(r)=f(r)-f(r_c)-(r-r_c)\left.\frac{df}{dr}\right|_{r_c}, \quad (13)$$

where f is generic and f_c represents the function actually used in the final fitted Hamiltonian.

The various parameters of our Hamiltonian are obtained by a nonlinear least-squares fit, using a Monte Carlo simulated annealing approach to minimize the following least-squares objective function, F:

$$F=\sum_{i=1}^{\#types}\sum_{j=1}^{\#members}\left[(E_{VB}^{i,j}-E_{LDA}^{i,j})^2+A\left(\frac{\partial E_{VB}^{i,j}}{\partial|q|_i}\right)^2\right], \quad (14)$$

where the sum runs over the number of types (7) corresponding to fcc, bcc, sc, DC, Gr.(Gr.), Gr.(BN), and chain, and over the number of members of these types (19, 8, 6, 35, 36, 7, and 4, respectively). E_{LDA} represents the *cohesive* energy as obtained by LDA calculation. The derivative with respect to charge is included in order to ''regularize'' the fit, i.e., to insure the fit obeys known physical and mathematical restraints. We set A, somewhat arbitrarily, to 0.05 but we find this value suffices. Note that the derivative with respect to q has a single superscript i. We define a single charge per structure type. Since these are 1:1 stoichiometry AB systems within our VB formalism, the charge on A is equal in magnitude to that on B; hence we need only concern ourselves in the fitting procedure with the absolute magnitude of this charge. This much simplifies the fitting procedure. [We also set the value of q equal for both the Gr.(Gr.) and Gr.(BN) structures. For Gr.(Gr.), there are actually two distinct sites in the unit cell which could be assigned different charges. Again, for simplicity, we set these equal.] In principle, the fit could be improved by having a different $|q|$ for each member of each structure type.

We imagine, in using this Hamiltonian for simulation, that the charges as well as the atomic positions will be dynamical variables. In principle the charges should be chosen for each atomic configuration such that the Hamiltonian is minimized. In practice, however, a method similar to that advocated by Sprik and Klein,[33] in their simulation of polarizable ammonia, could be used. Here, a fictitious Lagrangian with both positions and charges as dynamical variables is defined. The latter are given small masses and thermostated at $T=0$ so that they follow a close to minimum energy path as the nuclear positions change. In Eq. (6), we have implicitly as-

TABLE IV. LDA energy database for face centered, body centered, and simple cubic structures. Energy given in rydbergs (1 Ry=13.6057 eV; 1 eV=96.487 kJ/mole) per unit cell. Distances in bohr (1 bohr=0.5292 Å). One atom/cell.

a_1	Energy
fcc	
3.40	−73.630888
3.60	−74.117360
3.80	−74.470111
4.00	−74.725308
4.20	−74.908302
4.40	−75.038282
4.60	−75.129459
4.80	−75.193404
5.00	−75.237540
5.40	−75.282101
5.60	−75.288850
5.70	−75.289538
5.80	−75.288971
5.90	−75.286988
6.00	−75.283651
6.20	−75.273964
6.60	−75.246447
7.00	−75.212836
7.40	−75.177557
bcc	
2.80	−73.942855
3.40	−74.996865
3.90	−75.256660
4.30	−75.308258
4.40	−75.309672
4.50	−75.307974
4.60	−75.303841
4.90	−75.282560
sc	
2.40	−74.694901
2.70	−75.198740
3.10	−75.418211
3.40	−75.432528
3.70	−75.394521
3.90	−75.356841

TABLE V. LDA energy database for diamond cubic structure and simple tetragonal and orthorhombic distortions. Energy given in rydbergs per unit cell. Distances in bohr. Two atoms/cell.

a_1	a_2	a_3	Energy
5.80000			−150.997145
5.90000			−151.062386
6.00000			−151.116265
6.10000			−151.159919
6.20000			−151.194377
6.30000			−151.220635
6.50000			−151.251905
6.60000			−151.258347
6.67500			−151.259724
6.80000			−151.256150
7.00000			−151.237460
7.10000			−151.223113
7.20000			−151.205964
7.591643	5.314150		−151.109161
7.261145	5.808916		−151.191636
6.981589	6.283430		−151.242173
6.856891	6.514046		−151.254634
6.786196	6.650472		−151.258063
6.718330	6.785513		−151.258522
6.631911	6.963506		−151.254761
6.529865	7.182852		−151.243194
6.343195	7.611833		−151.199087
6.176190	8.029047		−151.130417
6.83598	6.64532	6.74200	−151.257744
6.89138	6.58992	6.74402	−151.256299
6.95381	6.52749	6.74740	−151.253896
7.04210	6.43920	6.75416	−151.249107
7.10985	6.37145	6.76093	−151.244336
7.21729	6.26401	6.77452	−151.234862
7.32441	6.15689	6.79159	−151.223125
7.41472	6.06659	6.80874	−151.211501
7.69392	5.78738	6.87821	−151.166916
7.90816	5.57314	6.94912	−151.124724
8.08878	5.39252	7.02151	−151.085908
8.24791	5.23339	7.09542	−151.050293

sumed a 50/50 weighting of degenerate representations of the system. In the discussion in Sec. IV below, we shall see that this weighting could be changed in a dynamical simulation so that the mean charge on each atom is not identically zero. This will be particularly useful when there is an applied electrostatic field. Such will be possible by generalizing the determinantal representation given in Eq. (1) above.

The database (see Tables II, III, IV, and V) as suggested in Eq. (14) was generated by a full-potential linearized augmented plane-wave (LAPW) code[34,35] with additional local orbitals in the basis set.[36] We used the Vosko-Wilk-Nusair[37,38] parametrization to represent the local-density approximation of the exchange-correlation potential. In each lattice we used a regular k-point mesh (including the Γ point) of sufficient density to insure energy convergence to about 0.005 eV/atom. For the insulating diamond structure, this involves 19 k points in the irreducible part of the Brillouin zone. For the semimetallic graphite structure we need 148 k points in the irreducible part of the Brillouin zone. We controlled the basis set size by setting

$$G_{max}=8.5/R_{mt}, \tag{15}$$

where G_{max} is the length of the longest reciprocal lattice vector used to construct the LAPW basis and R_{mt} is the muffin-tin radius assigned to each carbon atom. We used $R_{mt}=1.2$ bohrs (1 bohr$=5.292\times10^{-2}$ nm), yielding a basis of at least 100 functions per atom even at the smallest volumes used in the data base.

Such a scheme should be good at obtaining relative energies not only within structure types but also across these

TABLE VI. Final parameters for E_{VB}.

Parameter	Value	Parameter	Value
α	$1.1099211955437\times10^{-01}$	q_0	$-1.0484137513669\times10^{+00}$
β	$1.5410881606389\times10^{-02}$	k_+	$-1.7367644275837\times10^{-01}$
σ_0	$8.3229466864889\times10^{-01}$	k_-	$3.5109965697114\times10^{-01}$
ρ_0	$2.9372373965752\times10^{+00}$	q_{fcc}	$2.3814711502526\times10^{-01}$
χ	$8.6740796488118\times10^{-01}$	q_{bcc}	$2.6114465150277\times10^{-01}$
λ	$2.8327902400620\times10^{+00}$	q_{sc}	$1.5806510728854\times10^{+00}$
η_ρ	$8.6740796488118\times10^{-01}$	q_{dc}	$2.6766881692369\times10^{+00}$
η_r	$8.0033414542172\times10^{+00}$	q_{gr}	$2.7780445412291\times10^{+00}$
η_b	$3.0151646931655\times10^{+00}$	q_{chain}	$2.8194966559386\times10^{+00}$
η_{++}	$1.1287885983356\times10^{+01}$	U_+	$3.9867292540778\times10^{-01}$
η_{--}	$5.2234855528247\times10^{+00}$	U_-	$1.4878555053137\times10^{+01}$
η_{+-}	$8.1609701251399\times10^{+00}$	γ	$4.4522385954466\times10^{+00}$
r_c	$6.0093752071775\times10^{+00}$	ϵ	$6.0183618437052\times10^{-01}$
δ	$8.4254069592310\times10^{-01}$	ν	$3.1544940894354\times10^{-01}$

condensed phase families, including the very small energy difference between the optimal geometries of diamond and graphite. Unfortunately, LDA gets the incorrect order of stability. Whereas experimentally the graphite is lower in energy by 0.0195 eV/atom (1.883 kJ/mole), the LDA finds in favor of diamond by 0.0122 eV/atom (1.181 kJ/mole). (We view this accuracy as impressive.) A uniform shift of 0.0318 eV/atom is therefore applied to the entire DC database to bring it in line with the experimental Gr./DC equilibrium energy difference. Further, a constant shift of 1021.535 eV (75.0814 Ry) per atom is applied to the entire database so that all energies are referenced to zero as the infinitely separated atom limit. In other words, the energies thereby become cohesive energies which is what is assumed in the form of E_{VB}. Also, both the DC and Gr. databases are now compatible with *experimental* cohesive energies. The equilibrium cohesive energy for graphite is 7.45 eV/atom. Note that LDA finds, in accord with experiment, that the Gr.(Gr.) structure is slightly lower in energy than the Gr.(BN) structure. The experimental lattice parameter of DC is 3.57 Å whereas LDA finds 3.53. Graphite is similarly well described: LDA finds $a_1=2.43$ and $a_3=6.7$ Å, whereas experiment finds 2.46 and 6.70, respectively. Again, we view the structural determination as impressive, particularly because, for graphite, the interplanar bonding is weak and LDA might be expected to do less well. Indeed, we give only one decimal place accuracy for the interplanar separation because the energy minimum along this ordinate is so shallow. Last, within our data base for the DC and Gr. structures, lattice parameters which break the symmetry of the ideal lattice are included so that E_{VB} contains elastic constant information. Unlike the cohesive energies, we chose not to shift the lattice parameters of our LDA database to bring them into line with experiment—we view them as good enough as they are. The sum of all considerations made in this paragraph is what constitutes E_{LDA} as defined in Eq. (14).

Table VI gives the final fitted parameters. This fit represents the best of many optimizations with different starting points and different annealing schedules. Note that energies are in eV, distances are in angstroms, and the charge is given in atomic units. The constant K in Eq. (8) converts the long-range Coulomb term to electron volts and has the value $2\times13.6057\times0.5292=14.4003$ eV Å. The fcc system does not have a simple two component system with which to map—there is no AB system in which both the A and B atoms are twelvefold coordinated with the opposite species. However, there are a few common lattices which are fcc overall. There is the idealized $L1_0$ (TiAl) structure which is an AB system with 1:1 stoichiometry in which each atom has four nearest neighbors of its own kind and eight of the other. There is the idealized $L1_1$ structure which is also an AB system with 1:1 stoichiometry but now each atom has six neighbors of its own kind and six of the other. And finally, there is the Cu_3Au structure which has a 3:1 stoichiometry. Each Au atom has twelve Cu neighbors and each Cu atom has four Au and eight Cu neighbors. We find that of these three structure types, it is the TiAl structure which has the lowest Coulomb energy; the other two are much higher. (There are two other fcc structure types: the Al_3Ti and the Al_3Zn. We did not consider these. It is unnecessary; the Coulomb energy is so high that it does not contribute to E_{VB}.) Thus it is the TiAl structure that we use to represent fcc in fitting to our database. The fit describes each structure well. As expected, most of the weight for the metallic fcc and bcc structures is in the EAM term whereas for the DC, Gr., and chain structures it is in the ionic part of the VB Hamiltonian. The sc structure marks the crossover from the EAM to the VB ionic description but, in contrast to our LDA calculations which show the structure to be metallic, it is the Coulomb term which carries the most weight here. The Coulomb contribution is ~2 eV/atom lower than that of the EAM. Last, as anticipated from our ideas about radius ratios, for the DC and Gr. structures, the Coulomb energy is significantly lower than that of the EAM: by ~5 eV/atom.

Some other comments are in order about the fit. The ionic charge on carbon for the DC and Gr. structures is very similar—this occurs naturally with no applied constraint. This fact lends credence to the intrinsic insight of the model, namely that diamond and graphite are on the cusp of stability between fourfold and threefold coordination dictated by ionic radius ratios. The ionic charges of 2.68 and 2.78, re-

spectively, for the DC and Gr. structures produce effective cation hard-core radii [as defined by the σ in Eq. (9)] of 0.37 and 0.35 Å and anion radii of 1.77 and 1.81 Å. These produce radius ratios for these structures of 0.21 and 0.19 which are near the value of 0.22 suggested by Table I. As expected, for the fcc and bcc structures, the ionic charges are small, whereas that of the linear chain is large. Chemical intuition would predict that the latter structure might be dynamically stable. Indeed, MD with the present potential shows such to be true. However, the linear form of carbon does not occur naturally in nature, it being thermodynamically less stable than either diamond or graphite. The charge for the linear structure is very similar to that of Gr. resulting in a radius ratio of 0.19 which is larger than that predicted by Table I. However, Pauling's radius ratio[27] rules pertain *only* to stable structures.

The only part of the fit which is unphysical is the value of the electron affinity and ionization potential as suggested by Eq. (7). The experimental first electron affinity for carbon is near 1.2 eV and the first three ionization potentials are 11.3, 24.4, and 47.9 eV. Thus the value for q_0 of -1.05 a.u. found in the fit is near what we would expect; it is the charge at which the energy versus charge ''parabola'' is at a minimum. However, the fit produces, for the DC and Gr. structures on-site energies, ϕ_+ and ϕ_-, of ~ 5.2 and ~ 42 eV/atom, respectively. Given that the fitted charges in DC and Gr. are 2.68 and 2.78, respectively, the fitted on-site ionization energy should be much larger than the electron affinity. The *sum* of the two is the correct order of magnitude, however, and it is this sum that affects the overall E_{VB} energy. Unfortunately, U_+ and U_- cannot be adjusted retroactively to maintain a constant sum for the on-site energies while producing a more reasonable set of ionization energies and electron affinities since derivatives of these terms with respect the $\{q\}$ are also part of the fit [see Eq. (14)]. Nevertheless, with this one caveat, the resulting fit as we shall show below has proven to have good predictive power and transferability for many situations in carbon molecules and crystals.

In examining the derivatives of E_{VB} with respect to the charge q, the final fit produces respectably small values for all members of the database, but particularly so for the equilibrium geometries of the DC and Gr. structures. Indeed a sensitive way to determine the equilibrium geometry of the final fit is not only to look for the minimum in E_{VB} but also for the structure with the smallest derivative with respect to charge. The rms error for the energy of the entire database is 0.18 eV/atom while the RMS error for the derivative of the energy with respect to the charge is 0.76 eV/a.u. While this latter value might seem large, the variation of the energy with q, for values of q slightly different from the optimal, is extremely rapid. If the computational expense of optimizing q for *every* member of the database had been tractable, the rms error of the derivative would have been significantly lower.

The fitted value of r_c of 6.01 Å coupled with Eq. (13) ensures that there are no demanding long-range sums to compute. In fact, our original fit included an exponential damping term which multiplied the long-range Coulomb potential of Eq. (8) but it transpired that the use of Eq. (13) was so efficient that the damping coefficient had no discernible effect on the final fit. We have therefore omitted it from both Eq. (8) and Table VI.

TABLE VII. Comparison of equilibrium experimentally augmented LDA cohesive energies (eV/atom) and lattice parameters (angstroms) with those predicted by E_{VB}.

Structure	E_{LDA}	$\{a\}_{LDA}$	E_{VB}	$\{a\}_{VB}$
FCC	-2.83	3.02	-2.81	3.02
BCC	-3.11	2.33	-2.80	2.38
SC	-4.77	1.80	-4.54	1.80
DC	-7.43	3.53	-7.38	3.46
Gr.	-7.45	2.43/6.7	-7.73	2.41/7.64
Chain	-6.18	1.275	-6.09	1.30

Table VII compares the equilibrium cohesive energies and lattice parameters from our experimentally adjusted database to those predicted from the fit. Our Hamiltonian does remarkably well over the entire range of structures. It captures the energy versus bond-length relationships (not shown: a figure containing all the structures is too complex) very well. It also obtains a slightly lower energy (by ~ 0.1 eV/atom) for the Gr.(Gr.) structure than the Gr.(BN) structure. If there is a deficiency in the functional forms chosen for the fit, it is probably the EAM term: it has trouble differentiating between the energies of the fcc and bcc structures although it does obtain their lattice parameters well. Future work will focus on improving this. E_{VB} predicts the energy of the DC structure very well. On the other hand it predicts too low an energy for Gr. by approximately 0.3 eV/atom. Also, it obtains too large an interbasal plane spacing for Gr. This is the ''soft'' direction which competes with the much harder in-plane bonds. Given the nature of our Hamiltonian, we still view this ability to describe both ''chemical'' and ''physical'' bonds simultaneously as impressive.

The next section describes other implications of the Hamiltonian including the dynamical stability of the graphite and diamond systems as well as the thermodynamic stability of linear versus ring carbon molecules.

III. HAMILTONIAN PREDICTIONS

Our first prediction concerns the dynamical stability of the diamond and graphite systems. We employ a constant temperature, constant pressure algorithm which allows for flexible computational cell lengths and angles. The algorithm is described fully elsewhere.[39] Figures 1 and 2 show the energy and density of these systems as a function of temperature at a pressure of 1 atmosphere. The DC structure is completely stable up to the highest temperatures (4500 K) studied. This is near the temperature at which experimental carbon melts.[3] The Gr. structure is stable up to 2500 K at which point the basal planes start to move freely over one another. At approximately 3900 K the Gr. phase melts to a disordered structure; this is the system's attempt to produce liquid carbon (recall that the present code will bias against frustrated systems). We note that E_{VB} also produces a graphitic structure which is almost exactly of equal energy to the perfect Gr. stacking. This structure is not the BN stacking, but in-

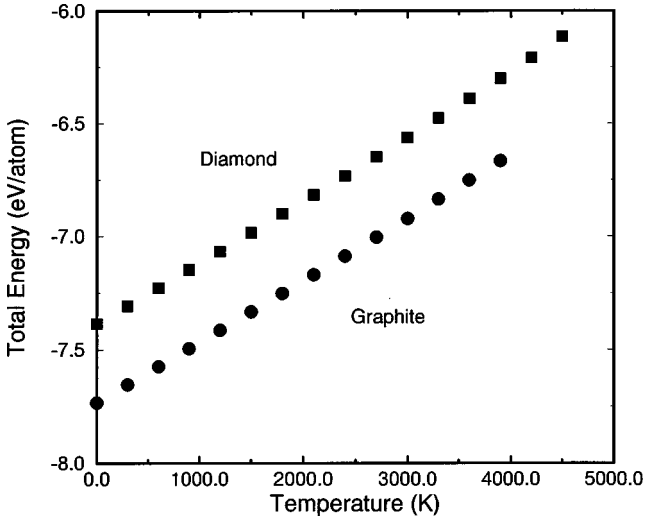

FIG. 1. Total (kinetic plus potential) energy as a function of temperature at a pressure of one atmosphere.

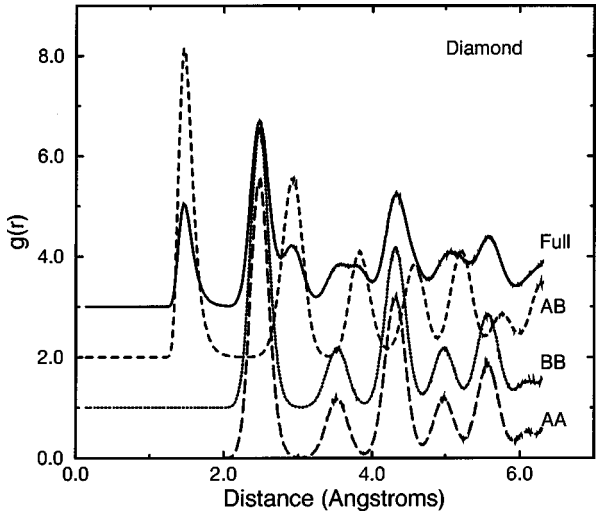

FIG. 3. Radial distribution function of diamond at 2400 K. The ''*AA*,'' ''*BB*,'' and ''*AB*'' components are also shown (see text).

volves atoms in one basal plane layer sitting above the carbon-carbon bonds of the layer below. Although there are no reports of such structures in the literature, different forms of graphite other than the ideal, which depend upon method of preparation, do exist.[40] Such forms differ from the ideal only in the basal plane stacking. Figure 2 can be used to predict a linear thermal-expansion coefficient α of 8.3 $\times 10^{-6}$/K for diamond and 1.4×10^{-6}/K for graphite. These numbers are difficult to compare to experiment, especially for diamond. The Debye temperature of diamond is on the order of 2000 K.[41] Thus quantum effects are very important experimentally, and we can only hope to compare our results to the high-temperature limit of α. This, too, is difficult, because the available experimental data for diamond only goes up to 1600 K,[42] i.e., below the Debye temperature and well below the asymptotic region. Using this data and the experimental behavior of the specific heat[43] we estimate the high-temperature thermal expansion coefficient of diamond to be between 6 and 7×10^{-6}/K. We consider this to be in good agreement with our simulation. The experimental situation for graphite is rather simpler. Data for α are known up to approximately 3000 K,[44] and at this point α is nearly saturated at a value of about 7.2×10^{-6}/K. This is much larger than the value obtained in our experiment. Last, Figs. 3 and 4 show the radial distribution functions of DC and Gr. at 2400 K. These functions are also decomposed into their ''*AA*,'' ''*BB*,'' ''*AB*'' components. Note that, as expected, the ''*AA*'' and ''*BB*'' contributions are identical.

Our second prediction concerns the stability of the lower homologues of C_n molecules. High quality first-principles calculations, which include many-body perturbative corrections beyond Hartree-Fock,[16] indicate that even number atom molecules should form rings, while odd numbered atom systems should form chains. The existing empirical potentials previously described would have great difficulty in duplicating such behavior. However, in the case of the present Hamiltonian in which the EAM contribution for low coordination numbers is weak and in which identities (either *A* or *B*) must necessarily be assigned in an alternating fashion along the chain in order to keep the Coulomb energy low, it

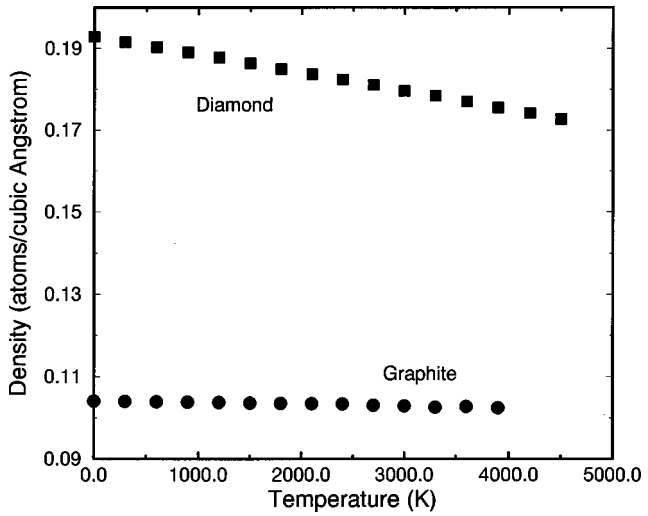

FIG. 2. Density as a function of temperature at a pressure of one atmosphere.

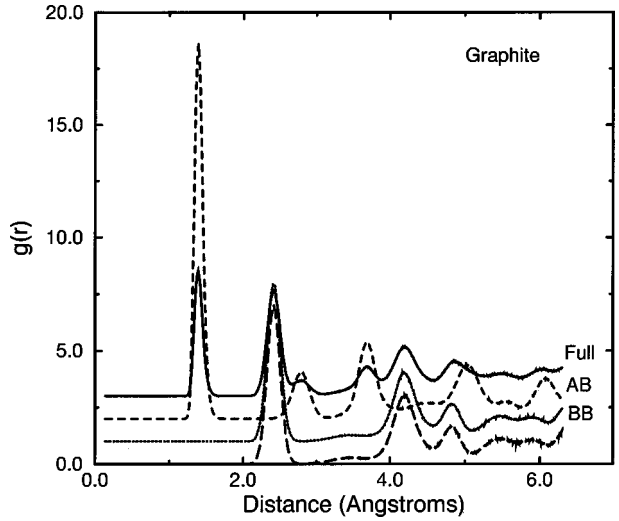

FIG. 4. Radial distribution function of graphite at 2400 K. The ''*AA*,'' ''*BB*,'' and ''*AB*'' components are also shown (see text).

TABLE VIII. Comparison of equilibrium structures and energies of C_5 and C_6 clusters as predicted from first-principles calculations[16] and from E_{VB}. Energies in eV/atom and distances in angstroms. Distances and charges (of the VB Hamiltonian) ordered with central atom/bond rightmost. ''Frustrated'' neighboring atoms in pentagonal C_5 have smallest charge. Bond angles in the E_{VB} ring structures are not optimized and are maintained as ideal; first-principle calculations show the C_6 ring structure to comprise nonideal angles. ''HFMP'' implies Hartree-Fock plus Moller-Plesset level of theory. The energy of linear C_6 is not given to high precision in Ref. 16.

Structure	E_{HFMP}	$\{r\}_{HFMP}$	E_{VB}	$\{r\}_{VB}$	$\{q\}_{VB}$
C_5 pentagon			−2.582	1.40	1.15, 2.2, 2.1
C_5 chain	−4.892	1.271, 1.275	−4.162	1.32, 1.31	2.05, 2.6, 2.7
C_6 hexagon	−4.948	1.316	−5.094	1.33	2.55
C_6 chain	−4.8		−4.485	1.32, 1.31, 1.31	2.05, 2.6, 2.7

is simple to see why even atom systems form rings and why odd atom molecules form chains. In the case of the former, identities can be assigned without ''frustration'' whereas in the latter case, a ring necessarily causes two like charges to be adjacent. Odd atom systems prefer to maximize the distance between such unfavorable interactions by forming a chain. In order to determine the energetics of a C_n ring, where n is odd, it is necessary to average over several degenerate representations corresponding to the n different ways of placing the unfavorable interactions around the ring. The exact way in which this is done is described in the next section which discusses the handling of frustrated systems.

Table VIII gives the predictions of the E_{VB} Hamiltonian and compares them with the high quality quantum chemical calculations of Raghavachari and Binkley[16] for C_5 and C_6. The present Hamiltonian correctly predicts that odd-member molecules are chains and even-membered systems form rings. The bond lengths of our Hamiltonian are a little longer than those obtained from first principles calculations. Further, the energy difference between chains and rings is larger than Raghavachari and Binkley calculate, although it seems that the present Hamiltonian does extremely well at predicting the cohesive energies of even-membered ring structures. Note that, for cyclic C_5, the ''frustrated'' charges which neighbor one another are, as expected, small. There is a tradeoff between their mutual repulsion if this charge is large and the reduction of the attraction to their other neighbors if it is too small. The energy of the C_5 ring predicted by E_{VB} is very different from the linear form. Unfortunately, an energy for the cyclic form is not given in Ref. 16. Nevertheless, given that these C_5 and C_6 molecules were not in our data base, the VB Hamiltonian behaves well.

IV. HAMILTONIAN GENERALIZATION AND CONCLUSIONS

We have seen that the Hamiltonian represented by Eq. (1) works well for highly symmetric, nonfrustrated systems. Such a formalism is expected to work well for other sp bonded single component systems, such as silicon. In the language of the present model, the reason why silicon does not form graphitic structures is because its effective cation/anion radius ratio is not near the value 0.225 (see Table I) separating fourfold from threefold coordination. Rather, the value is firmly in the fourfold region. Further, because of the proximity of near lying d states and the narrowness of its band gap relative to carbon, the EAM contribution will be more significant in the determinantal representation of the energy, E_{VB}. This latter contribution favors higher coordination.

Turning now to elements in the middle of the d block where metallic bonding as well as covalency is important (e.g., those elements forming bcc structures), the present formalism may again be useful. Simple EAM descriptions are known to handle such systems with difficulty. However, the present treatment, which allows a mixing of EAM and Coulomb descriptions, is expected to work better. The effective radius ratio rules will now place the element in the range where eightfold coordination is favored. The ionic and EAM contributions in the determinantal representation of the energy will strongly couple; that is, the off-diagonal terms will be important.

Last, two-component systems, such as SiC, should also benefit from such a description. The exact degeneracy of competing charge distributions will now be lifted, but nevertheless the same VB treatment should still pertain. Even a material exhibiting as much charge transfer as GaAs should benefit from the VB description since the EAM term, just as in the discussion above for Si, is likely to have nonzero weight. It remains to be seen whether explicit introduction into the Hamiltonian of charge distributions which are allowed to ''float'' off atomic centers, much in the same way that quantum chemists[45] use floating Gaussians to improve their bases, will be necessary.

Turning now to systems exhibiting frustration, how might such a representation be generalized for more complex situations? VB methods have the drawback of a combinatoric explosion: in principle, all possible ways of assigning charge distributions to atoms within the system should contribute to the Hamiltonian. Hopefully, if this general approach is to be useful for simulation, only a small number of these actually carry much weight. In the case of systems like C_5 or C_{60} (which has five membered rings), the number of important degenerate representations is low and we expect that generalization of our Hamiltonian will be computationally tractable.

Returning to Eq. (1), a better determinantal expression for the energy of highly symmetric nonfrustrated systems is:

$$\begin{vmatrix} (H_E - E_{VB}) & (H_{EC_1} - E_{VB}S_{EC_1}) & (H_{EC_1} - E_{VB}S_{EC_1}) \\ (H_{EC_1} - E_{VB}S_{EC_1}) & (H'_{C_1} - E_{VB}) & (H_{C_1C_2} - E_{VB}S_{C_1C_2}) \\ (H_{EC_2} - E_{VB}S_{EC_2}) & (H_{C_2C_1} - E_{VB}S_{C_2C_1}) & (H'_{C_2} - E_{VB}) \end{vmatrix} = 0, \tag{16}$$

where C_1 and C_2 represent the two degenerate charge distributions within Eq. (6). H'_C is no longer the mean of these degenerate states, but is the Coulomb energy of a given charge distribution. H_E remains as before. In the absence of a field, we expect that the overlap between these two degenerate representations would be zero; that is we expect the off-diagonal $H_{C_1C_2}$ and $S_{C_1C_2}$ terms to be zero. Thus the following forms for S and H suggest themselves for the case where there are P degenerate contributing VB states and the charges in each state are allowed to be dynamical variables:

$$S_{EC_n} = (P^{-1/2}) e^{-\gamma \sqrt{1/N \sum_i (q_i^{C_n})^2}},$$

$$H_{EC_n} = \frac{\varepsilon_{EC_n}(\{q\})}{2} (H_E + H'_{C_n}) S_{EC_n} e^{-\delta/N |H_E - H'_{C_n}|},$$

$$S_{C_nC_m} = \delta_{nm},$$

$$H_{C_nC_m} = \delta_{nm} H'_{C_n}. \tag{17}$$

C_n and C_m represent states of given charge distribution. Index i runs over all atoms in the system. The pre-exponential factor in S_{EC_n} is a required normalization for a Hamiltonian with P degenerate contributing ionic VB states. Since the $\{q\}$ are now dynamical variables, both ε and H'_C have to be defined more generally than before:

$$\varepsilon_{EC_n}(\{q\}) = 1 + \epsilon \sqrt{\frac{1}{N} \sum_i (q_i^{C_n})^2},$$

$$H'_{C_n} = \sum_i (H_i^{C_n})',$$

$$(H_i^{C_n})' = H_i^E e^{-\nu |q_i|} + H_i^{C_n} (1 - e^{-\nu |q_i|}). \tag{18}$$

Here it is necessary to define an energy for each atom. This may be done in intuitive fashion by examining Eqs. (3) and (6). The above Eqs. (17) and (18) both reduce to those given earlier when there was only one value of $|q|$ per state.

In the case of nonfrustrated systems, a 3×3 determinant for the energy is likely to behave well and be computationally efficient. Such would be the case, for example, for fullerene tubules in which there are no five or seven membered ring defects. A good description at finite temperatures may require dynamical charges. In contrast, for frustrated systems of high symmetry, the determinant is larger. Here, the number of equivalent states is known exactly and the determinant can be written out in its entirety. The size of the determinant, however, depends upon what assumptions are made about the contributing ionic states. For example, in the case of a C_5 ring, if the ''*AB*/*BA*'' representation used in the earlier sections is enforced, the determinant would be 11×11 (i.e., the EAM state plus the 2×5 degenerate charges states). However, if this constraint is removed, then the determinant would be 6×6 (i.e., the EAM state plus the five degenerate ways of cyclically permuting atomic charges). It remains to be seen which representation is the more accurate. (The results quoted in the prior section for pentagonal C_5 used the 11×11 determinant.) In either case, those frustrated atoms which have like neighboring polarity will lower their energy by reducing their ionic charge.

Turning now to systems of low symmetry, such as liquids, there could potentially be a combinatoric explosion of different contributing VB states. Unfortunately, C_{60} is in this class also. The number of contributing ionic states in its degenerate manifold is extremely large. However, it may well be that only a finite number of such states are important to describe the energetics of these systems quite accurately. We anticipate this because, for any configuration, the total energy of the system is being minimized with respect to all the $\{q\}$ dynamical variables in the system. There are $(N \times P)$ of these. As in the case of tight-binding moment methods for liquids,[46] where the number of moments is increased, or path-integral quantum simulations,[47] where the number of imaginary time slices is increased, an approach in which the number of contributing states is increased until there are no further changes in the system properties would be an appropriate way to proceed. Notice that even here, the computational complexity would scale as $O(N)$, albeit with a significant prefactor. However, even with this prefactor, the method should still be much faster than tight-binding and *ab initio* methods. The important ionic states are almost certainly not degenerate representations and thus H_{CC} and S_{CC} terms now contribute to the E_{VB} Hamiltonian. Continuing in similar vein to Eqs. (17) and (18), these terms should have the form

$$S_{C_nC_m} = e^{-\gamma \sqrt{1/N \sum_i (q_i^{C_n} - q_i^{C_m})^2}},$$

$$H_{C_nC_m} = \frac{\varepsilon_{C_nC_m}(\{q\})}{2} (H'_{C_n} + H'_{C_m}) S_{C_nC_m} e^{-\delta/N |H'_{C_n} - H'_{C_m}|},$$

$$\varepsilon_{C_nC_m}(\{q\}) = 1 + \epsilon \sqrt{\frac{1}{N} \sum_i (q_i^{C_n} - q_i^{C_m})^2}. \tag{19}$$

The expressions for S_{CC} and H_{CC} reduce to the same form as those of S_{EC} and H_{EC} when one recognizes that the EAM state has zero effective charge on each atom. Note that the definition of S_{CC} in Eq. (19) does not equal zero between

states in a degenerate manifold, but the value of the overlap exponent γ is sufficiently large that such concerns may be academic.

When q_i is a dynamical variable one or more constraints will be necessary. For example, charge conservation in each contributing state is required. It may also be necessary to introduce, particularly for systems of low symmetry, overall charge neutrality (in the absence of an external field) upon each atom. Such constraint might be either hard or soft. Perhaps a constraint that imposes uniform charge-charge correlations across the system would also be useful. As noted in the Introduction, a computationally efficient way to deal with extra degrees of freedom would be to use the fictitious Lagrangian method advocated by Sprik and Klein[33] in their study of polarizable liquid ammonia.

Finally, when simulating a system in the presence of an external field, although each contributing state, whether it be ionic or EAM, couples to the field, the weight of the ionic terms is so great for the systems of low coordination when using this Hamiltonian, that merely coupling the ionic charges to the external field may suffice to capture most of the important physics. Certainly atomic charges, if they are allowed to be dynamical variables, will redistribute in response to the field. For example, if a fullerene tubule with no five or seven membered rings is to be simulated in the presence of an external field, a (3×3) determinant representation, in which the ''AB/BA'' charge equality constraint has been removed, would probably describe the energetics very well.

In conclusion, we have developed an interatomic potential for carbon, which may easily be generalized to other covalent systems such as silicon, silicon carbide, or even mid *d*-block transition elements. Unlike potentials based upon molecular orbital ideas, the functional form does not involve angular terms; it is based upon concepts rooted in valence bond theory. We have shown that it is capable of stabilizing both the diamond and graphite structures and that it has remarkable predictive power for small carbon clusters. It is computationally very efficient for high-symmetry, nonfrustrated systems. We have suggested a way forward for more complex systems such as liquids and fullerene systems with five and seven member rings. We emphasize that even for the low symmetry systems where many important ionic states may be required in the Hamiltonian, the approach still scales as $O(N)$. The ideas introduced in this final section are the subject of ongoing work.

ACKNOWLEDGMENTS

J.Q.B. and M.J.M. wish to acknowledge support of the ONR. J.Q.B. would like to thank the NSF and the ITP at Santa Barbara for support and hospitality during the spring of 1997.

[1] M.T. Yin and M.L. Cohen, Phys. Rev. Lett. **50**, 2006 (1983).
[2] S. Fahy and S.G. Louie, Phys. Rev. B **36**, 3373 (1987).
[3] G. Galli, R.M. Martin, R. Car, and M. Parrinello, Phys. Rev. Lett. **63**, 988 (1989); Science **250**, 1547 (1990).
[4] G. Galli, R.M. Martin, R. Car, and M. Parrinello, Phys. Rev. Lett. **62**, 555 (1989); Phys. Rev. B **42**, 7470 (1990).
[5] A.A. Quong, M.R. Pederson, and J.L. Feldman, Solid State Commun. **87**, 535 (1993).
[6] J.L. Feldman, J.Q. Broughton, L.L. Boyer, D.E. Reich, and M.D. Kluge, Phys. Rev. B **46**, 12 731 (1992).
[7] R.A. Jishi, R.M. Mirie, and M.S. Dresselhaus, Phys. Rev. B **45**, 13 685 (1992).
[8] B.L. Zhang, C.Z. Wang, and K.M. Ho, Chem. Phys. Lett. **193**, 225 (1992).
[9] J.Q. Broughton, J.V. Lill, and J.K. Johnson, Phys. Rev. B **55**, 2808 (1997).
[10] D. Porezag, M.R. Pederson, T. Frauenheim, and T. Kohler, Phys. Rev. B **52**, 14 963 (1995).
[11] J. Yu, R.K. Kalia, and P. Vashishta, J. Chem. Phys. **103**, 6697 (1995).
[12] P.R. Briddon and R. Jones, Physica B **185**, 179 (1993).
[13] S.A. Kajihara, A. Antonelli, and J. Bernholc, Physica B **185**, 144 (1993).
[14] G.B. Bachelet, G.A. Baraff, and M. Schluter, Phys. Rev. B **24**, 4736 (1981).
[15] K. Jackson, M.R. Pederson, and J.G. Harrison, Phys. Rev. B **41**, 12 641 (1990).
[16] K. Raghavachari and J.S. Binkley, J. Chem. Phys. **87**, 2191 (1987).
[17] F.H. Stillinger and T.A. Weber, Phys. Rev. B **31**, 5262 (1985).
[18] J. Tersoff, Phys. Rev. Lett. **56**, 632 (1986); Phys. Rev. B **37**, 6991 (1988); **38**, 9902 (1988).
[19] R. Biswas and D.R. Hamann, Phys. Rev. Lett. **55**, 2001 (1985); Phys. Rev. B **36**, 6434 (1987).
[20] J.R. Chelikowsky, J.C. Phillips, M. Kamal, and M. Strauss, Phys. Rev. Lett. **62**, 292 (1989).
[21] J.R. Chelikowsky and J.C. Phillips, Phys. Rev. B **41**, 5735 (1990).
[22] J.R. Chelikowsky, K.M. Glassford, and J.C. Phillips, Phys. Rev. B **44**, 1538 (1991).
[23] M.Z. Bazant, E. Kaxiras, and J.F. Justo, Phys. Rev. B **56**, 8542 (1997).
[24] D.W. Brenner, Phys. Rev. Lett. **63**, 1022 (1989); Phys. Rev. B **42**, 9458 (1990).
[25] D.G. Pettifor, in *Many Atom Interactions in Solids*, edited by R.M. Nieminen, M.J. Puska, and M.J. Manninen, Springer Proceedings in Physics Vol. 48 (Springer, New York, 1990).
[26] P. Alinaghian, P. Gumbsch, A.J. Skinner, and D.G. Pettifor, J. Phys.: Condens. Matter **5**, 5795 (1993).
[27] L. Pauling, *The Nature of the Chemical Bond*, 3rd ed. (Cornell University Press, New York, 1960).
[28] E.C. Behrman, R.K. Foehrweiser, J.R. Myers, B.R. French, and M.E. Zandler, Phys. Rev. A **49**, R1543 (1994).
[29] M. Wilson and P.A. Madden, Faraday Discuss. **106**, 339 (1997).
[30] M.S. Daw and M.I. Baskes, Phys. Rev. Lett. **50**, 1285 (1983).
[31] M.S. Daw and M.I. Baskes, Phys. Rev. B **29**, 6443 (1984).
[32] R.A. Johnson and D.J. Oh, J. Mater. Res. **4**, 1195 (1989).
[33] M. Sprik and M.L. Klein, J. Chem. Phys. **89**, 7556 (1988).
[34] O.K. Andersen, Phys. Rev. B **12**, 3060 (1975).
[35] S.H. Wei and H. Krakauer, Phys. Rev. Lett. **55**, 1200 (1985).
[36] D. Singh, Phys. Rev. B **43**, 6388 (1991).

[37] S. H. Vosko, L. Wilk, and M. Nusair, Can. J. Phys. **58**, 1200 (1980).
[38] S.H. Vosko and L. Wilk, Phys. Rev. B **22**, 3812 (1980).
[39] J.Q. Broughton, C.A. Meli, P. Vashishta, and R.K. Kalia, Phys. Rev. B **56**, 611 (1997).
[40] R.W.G. Wyckoff, *Crystal Structures* (Wiley, New York, 1963), Vol. 1.
[41] N.W. Ashcroft and N.D. Mermin, *Solid State Physics* (Holt, Rinehart and Wilson, New York, 1976), p. 461.
[42] G.A. Slack and S.F. Bartram, J. Appl. Phys. **46**, 89 (1975).
[43] Y.S. Touloukian and E.H. Buyco, *Thermophysical Properties of Matter* (IFI/Plenum, New York and Washington, 1970), Vol. 5.
[44] Y.S. Touloukian, R.K. Kirby, R.E. Taylor, and T.Y.R. Lee, *Thermophysical Properties of Matter* (IFI/Plenum, New York and Washington, 1977), Vol. 13.
[45] M.R. Pederson, B.M. Klein, and J.Q. Broughton, Phys. Rev. B **38**, 3825 (1988).
[46] M. Aoki, A.P. Horsfield, and D.G. Pettifor, J. Phase Equilib. **18**, 614 (1997).
[47] D.M. Ceperley, Adv. Chem. Phys. **93**, 1 (1996).